served that some *dpp-pka* mutant clones in the dorsal-anterior quadrant of the leg do not express WG. Possible explanations include the following: (i) repression by endogenous DPP, affecting clones located near the A-P boundary; or (ii) the combination of dpp^{H61} *pka-C1*^{h2} with *Tn(JA1, dpp*$^{+}$*)* does not behave as a complete loss of function for *dpp*. Clones of cells mutant for dpp^{H61} *pka-C1*^{h2} that carry *Tn(JA1, dpp*$^{+}$*)* exhibit some DPP activity, in that they have a low level of expression of *omb* in the wing. Comparable dpp^{H61} *pka-C1*^{h2} clones that lack the transgene do not express *omb* (*32*). For technical reasons, the clones examined here were generated in the presence of the *Tn(JA1, dpp*$^{+}$*)* transgene. Although not sufficient to repress WG in all cases, it is possible that the low level of DPP activity provided by the transgene prevents WG expression in some clones.

40. B. Cohen, A. A. Simcox, S. M. Cohen, *Development* **117**, 597 (1993).
41. M. van den Heuvel, R. Nusse, P. Johnston, P. A. Lawrence, *Cell* **59**, 739 (1989).
42. M. Frasch, *Nature* **374**, 464 (1995).
43. *H15 lacZ* expression was visualized by X-Gal staining. *Act5C>y*$^{+}$*>wg* is described in (*19*). Larvae of genotype *y HSFlp;Act5C>y*$^{+}$*>wg/H15-lacZ* were subjected to a 90-min heat shock at 38°C at 60 ± 12 hours of age (second instar). This treatment causes excision of the *flip*-out cassette (a segment of DNA bounded by direct FRT repeats) in virtually all cells, resulting in low-level ubiquitous WG expression. This level of WG expression is sufficient to direct *H15* expression but does not repress DPP expression (*20*). The *GAL30A* driver is described in (*29*). Larval genotypes: (Fig. 3C) *GAL30A/+; UAS-wg/+*; (Fig. 3D) *GAL30A/H15-lacZ; UAS-wg/+*; (Fig. 3E) *GAL30A/+; UAS-wg UAS-dpp/+*; and (Fig. 3F) *GAL30A/H15-lacZ; UAS-wg UAS-dpp/+*.
44. We thank C. Pfeifle for help in molecular characterization of *H15* and for isolation of *H15* mutants; A.-M. Voie for producing the WG monoclonal antibody; W. Norris and P. Ingham for mouse antibody to PTC protein; F. Diaz-Benjumea and V. Wiersdorff for sharing unpublished results; and S. Eaton, M. Averof, M. Ng, and an anonymous reviewer for suggesting improvements to the manuscript. W.J.B. is the recipient of an EMBO long-term fellowship in molecular biology.

13 May 1996; accepted 24 July 1996

Purification and Molecular Cloning of Plx1, a Cdc25-Regulatory Kinase from *Xenopus* Egg Extracts

Akiko Kumagai and William G. Dunphy

Cdc2, the cyclin-dependent kinase that controls mitosis, is negatively regulated by phosphorylation on its threonine-14 and tyrosine-15 residues. Cdc25, the phosphatase that dephosphorylates both of these residues, undergoes activation and phosphorylation by multiple kinases at mitosis. Plx1, a kinase that associates with and phosphorylates the amino-terminal domain of Cdc25, was purified extensively from *Xenopus* egg extracts. Cloning of its complementary DNA revealed that Plx1 is related to the Polo family of protein kinases. Recombinant Plx1 phosphorylated Cdc25 and stimulated its activity in a purified system. Cdc25 phosphorylated by Plx1 reacted strongly with MPM-2, a monoclonal antibody to mitotic phosphoproteins. These studies indicate that Plx1 may participate in control of mitotic progression.

In dividing eukaryotic cells, the entry into mitosis is governed by M phase–promoting factor (MPF). MPF, which consists of the Cdc2 protein kinase and cyclin B, acts by phosphorylating substrates that are essential for the execution of mitotic processes (*1*). Before mitosis, the activity of Cdc2–cyclin B is suppressed through phosphorylation of its Thr^{14} and Tyr^{15} residues by the Wee1 and Myt1 kinases (*2*). Cdc25, a dual-specificity phosphatase that dephosphorylates both Thr^{14} and Tyr^{15}, has a pivotal role in the cell cycle by activating Cdc2 at the G_2-M boundary (*3*, *4*). In higher eukaryotes, there are at least three members of the Cdc25 family (A, B, and C) that appear to act at different points in the cell cycle (*5*), but presently the role of Cdc25C in the G_2-M transition is best understood.

In *Xenopus*, Cdc25C (Xcdc25) undergoes extensive phosphorylation of its NH_2-terminal regulatory domain at mitosis (*3*, *4*). This phosphorylation strongly stimulates the Cdc2-specific phosphatase activity of Cdc25 and conceivably could have additional roles in its localization or stability. The NH_2-terminal region of Xcdc25, like that of Cdc25 proteins in other species, is rich in Ser-Pro and Thr-Pro motifs, which constitute part of the consensus recognition site for Cdc2 and other cell cycle–regulated kinases (*1*). Although Cdc2 appears to participate in the regulation of Xcdc25, there is at least one other mitotic kinase that phosphorylates Xcdc25 (*6*, *7*). In principle, this kinase or kinases could act upstream of Cdc2 to trigger its activation. Alternatively, it could act downstream of Cdc2 and thereby facilitate the progression through and eventual exit from mitosis.

One clue about the identity of this Xcdc25-specific kinase is that the phosphorylated form of Xcdc25 found at mitosis interacts strongly with the MPM-2 antibody (*8*). The MPM-2 antibody binds to a phosphopeptide epitope present in various mitotic phosphoproteins, including other regulators of mitosis such as Wee1, Myt1, NimA, and the anaphase-promoting complex (*2*, *9*). Thus, one or more kinases that phosphorylate the MPM-2 epitope are most likely to participate in mitotic control (*10*).

A major Xcdc25-specific kinase distinct from Cdc2–cyclin B (*7*) associated with exogenously added recombinant Xcdc25 in M-phase egg extracts from *Xenopus*. This kinase bound well to a histidine-tagged fusion protein containing the NH_2-terminal domain of Xcdc25 (His6-Xcdc25-N, residues 1 to 264) (*11*). We used a His6-Xcdc25-N affinity column and several conventional chromatographic steps (Superdex 200, phosphocellulose, and Mono Q) to enrich this Cdc25-specific kinase activity approximately 2500-fold (Table 1) (*12*). Upon separation of this highly enriched fraction in a sucrose density gradient, a 67-kD polypeptide (p67) comigrated closely with the kinase activity (Fig. 1) (*13*). We isolated several micrograms of p67 and sequenced four of its tryptic peptides (*14*). Polymerase chain reaction (PCR) primers designed for two of these peptides were used to amplify an 850–base pair (bp) segment of the cDNA encoding p67 (*15*). This fragment was used to isolate a full-length 2.4 kb cDNA encoding an open reading frame that contains all four tryptic peptide sequences (Fig. 2) (*16*). The complete amino acid sequence indicates that p67 is a typical

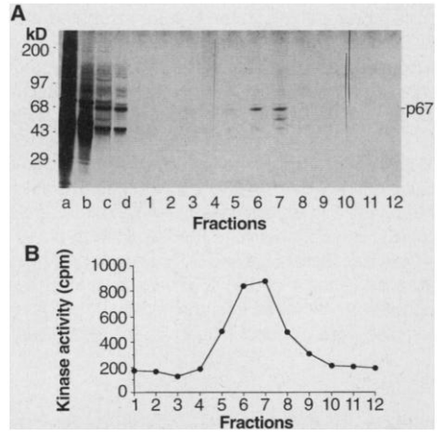

Fig. 1. Purification of a mitotic kinase that phosphorylates the NH_2-terminal domain of Xcdc25. (**A**) A cytosol fraction from an M-phase egg extract that had been eluted from a His6-Xcdc25-N agarose column (lane a) was subjected to chromatography on Superdex 200 (lane b), phosphocellulose (lane c), and Mono Q (lane d). The Mono Q fraction was separated in a sucrose gradient. Fractions from the columns and sucrose gradient (lanes 1 through 12, bottom to top) were subjected to SDS gel electrophoresis and silver staining. (**B**) Xcdc25-specific kinase activity of the sucrose gradient fractions.

Division of Biology, 216-76, Howard Hughes Medical Institute, California Institute of Technology, Pasadena, CA 91125, USA.

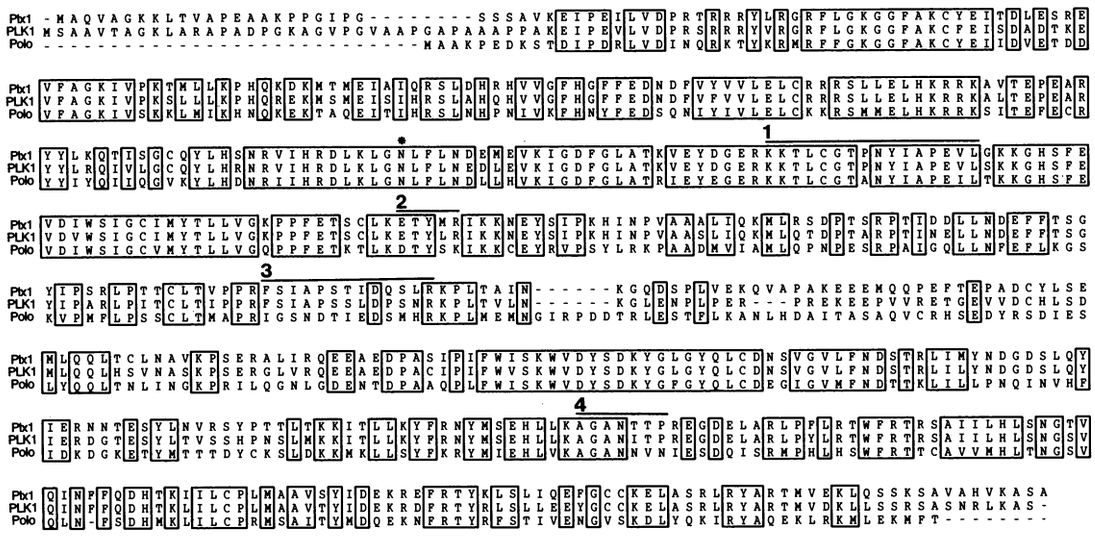

Fig. 2. Predicted amino acid sequence of Plx1 (*30*). The nucleotide sequence of the Plx1 cDNA (GenBank accession number U58205) contains an open reading frame of 598 amino acids that is preceded by three in-frame stop codons. The amino acid sequence of Plx1 was aligned (*2*) with those of human PLK1 (*17*) and *Drosophila* Polo (*18*). Residues conserved in all three kinases are boxed. The sequences corresponding to those obtained from tryptic peptide analysis of Plx1 are indicated by the lines above the sequence: peptide 1, KKXLX(T/G)TPNYIAPEVL; peptide 2, XXYM(T/R); peptide 3, XX(D/I)APSTIDQTLR; and peptide 4, (A/S)GANTTP. (Unreadable residues are indicated with an X and ambiguous residues are surrounded by parentheses.) The asterisk denotes the conserved asparagine that was mutated to alanine to create the catalytically inactive Plx1 N172A mutant.

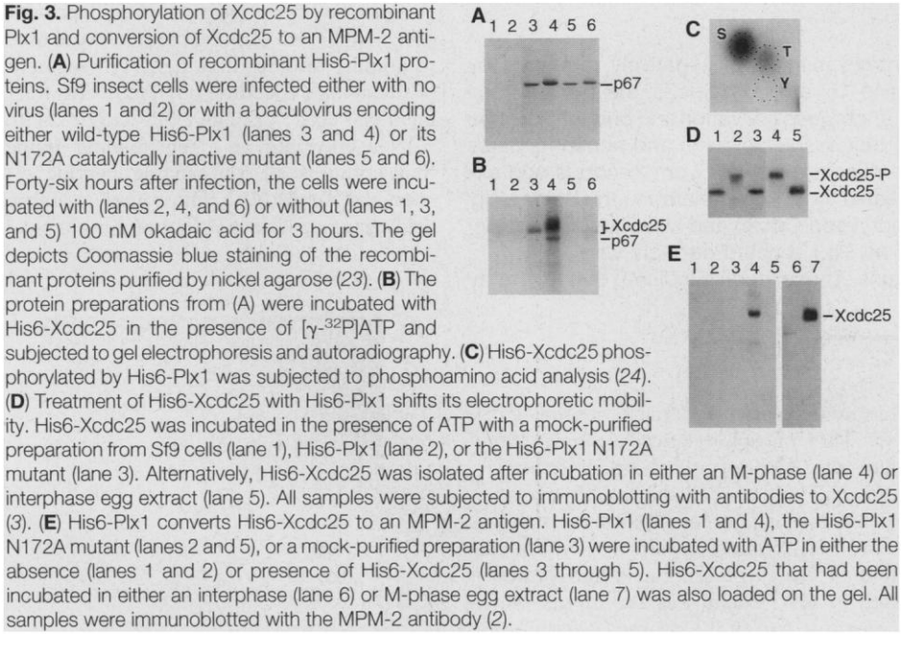

Fig. 3. Phosphorylation of Xcdc25 by recombinant Plx1 and conversion of Xcdc25 to an MPM-2 antigen. (**A**) Purification of recombinant His6-Plx1 proteins. Sf9 insect cells were infected either with no virus (lanes 1 and 2) or with a baculovirus encoding either wild-type His6-Plx1 (lanes 3 and 4) or its N172A catalytically inactive mutant (lanes 5 and 6). Forty-six hours after infection, the cells were incubated with (lanes 2, 4, and 6) or without (lanes 1, 3, and 5) 100 nM okadaic acid for 3 hours. The gel depicts Coomassie blue staining of the recombinant proteins purified by nickel agarose (*23*). (**B**) The protein preparations from (A) were incubated with His6-Xcdc25 in the presence of [γ-^{32}P]ATP and subjected to gel electrophoresis and autoradiography. (**C**) His6-Xcdc25 phosphorylated by His6-Plx1 was subjected to phosphoamino acid analysis (*24*). (**D**) Treatment of His6-Xcdc25 with His6-Plx1 shifts its electrophoretic mobility. His6-Xcdc25 was incubated in the presence of ATP with a mock-purified preparation from Sf9 cells (lane 1), His6-Plx1 (lane 2), or the His6-Plx1 N172A mutant (lane 3). Alternatively, His6-Xcdc25 was isolated after incubation in either an M-phase (lane 4) or interphase egg extract (lane 5). All samples were subjected to immunoblotting with antibodies to Xcdc25 (*3*). (**E**) His6-Plx1 converts His6-Xcdc25 to an MPM-2 antigen. His6-Plx1 (lanes 1 and 4), the His6-Plx1 N172A mutant (lanes 2 and 5), or a mock-purified preparation (lane 3) were incubated with ATP in either the absence (lanes 1 and 2) or presence of His6-Xcdc25 (lanes 3 through 5). His6-Xcdc25 that had been incubated in either an interphase (lane 6) or M-phase egg extract (lane 7) was also loaded on the gel. All samples were immunoblotted with the MPM-2 antibody (*2*).

Table 1. Purification of an Xcdc25-specific kinase from M-phase extracts of *Xenopus* eggs. The Xcdc25-specific kinase activity of each fraction was measured as described (*29*). The amount of protein was determined either by the Bio-Rad assay (Cytosol, His6-Xcdc25-N-agarose, and Superdex 200 fractions) or by silver staining (phosphocellulose and Mono Q fractions) with bovine serum albumin as a standard.

Fraction	Total protein (μg)	Total activity (nmol/min)	Specific activity (nmol/mg/min)	Purification (fold)
Cytosol	75,000	0.975	0.013	1
Xcdc25-N-agarose	1,200	0.548	0.457	35
Superdex 200	480	0.274	0.572	44
Phosphocellulose	5	0.019	3.715	286
Mono Q	0.2	0.006	30	2,308

serine-threonine kinase with its conserved catalytic domain in the NH_2-terminal half of the polypeptide. The p67 protein is very similar to kinases in the Polo family, including human PLK1 (80% identical residues with p67) (*17*), *Drosophila* Polo (53% identical) (*18*), *Schizosaccharomyces pombe* Plo1 (40% identical) (*19*), and *Saccharomyces cerevisiae* Cdc5 (37% identical) (*20*). Accordingly, we have designated p67 as Plx1 (for Polo-like kinase from *Xenopus*).

We expressed Plx1 as a six-histidine fusion protein (His6-Plx1) in baculovirus-infected Sf9 insect cells (Fig. 3A) (*21*). Because Plx1 activity is greater in mitotic than in interphase extracts from *Xenopus* eggs (*7*), we treated insect cells expressing His6-Plx1 with okadaic acid to drive them into a state resembling mitosis. We also expressed a mutant version of His6-Plx1 (N172A), in which a catalytically critical residue (Asn^{172}) was changed to alanine (*22*). Both the wild-type and N172A forms of His6-Plx1 were purified from insect cells by chromatography on nickel agarose (*23*) and incubated with recombinant His6-Xcdc25 in the presence of γ-^{32}P–labeled adenosine triphosphate ([γ-^{32}P]ATP). Wild-type His6-Plx1phosphorylated His6-Xcdc25 efficiently, whereas the N172A mutant did not (Fig. 3B). Phosphoamino acid analysis of the phosphorylated His6-Xcdc25 revealed the presence of both phosphoserine and phosphothreonine (Fig. 3C) (*24*). Phosphorylation of Xcdc25 with His6-Plx1 reduced the electrophoretic mobility of Xcdc25 substantially, which is characteristic of Cdc25 derived from mitotic cells (Fig. 3D). The N172A mutant had no effect (Fig. 3D). The shifted form of Xcdc25 also reacted with MPM-2

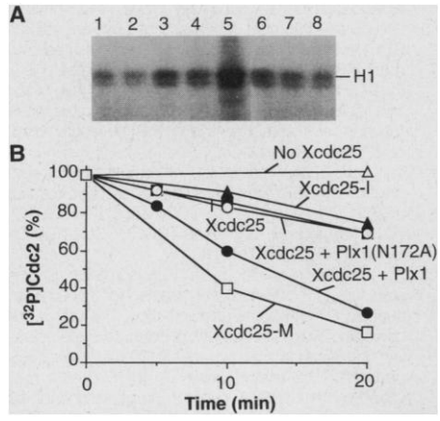

Fig. 4. Increased phosphatase activity of Xcdc25 after phosphorylation by His6-Plx1. (**A**) His6-Plx1 stimulates the ability of Xcdc25 to activate the Cdc2–cyclin B complex. His6-Δcyclin B (*28*) was incubated in interphase egg extracts containing 10 mM vanadate and cycloheximide (100 μg/ml). The resulting inactive Cdc2–cyclin B complex phosphorylated on Thr^{14} and Tyr^{15} was purified by nickel agarose and kept on ice (lane 1) or incubated at 23°C for 30 min by itself (lane 2). In lanes 3 through 8, samples containing His6-Xcdc25 (lanes 3 through 5) or lacking His6-Xcdc25 (lanes 6 through 8) were incubated for 30 min in the presence of a mock-purified preparation (lanes 3 and 6), the His6-Plx1 N172A mutant (lanes 4 and 7), or His6-Plx1 (lanes 5 and 8) before addition to the inactive Cdc2–cyclin B complex. At the end of the activation assay, H1 kinase activity was assessed by gel electrophoresis and autoradiography (*3*). (**B**) Dephosphorylation of the Thr^{14} and Tyr^{15} residues of Cdc2 by various forms of the His6-Xcdc25 protein. A Cdc2–cyclin B complex that had been labeled with ^{32}P by treatment with Myt1 (*2*) was incubated for the indicated times in the absence of His6-Xcdc25 (open triangle) or in the presence of His6-Xcdc25 that had been treated with His6-Plx1 (closed circles), the His6-Plx1 N172A mutant (open circles), a mock-purified preparation (closed squares), an interphase egg extract (closed triangles), or an M-phase egg extract (open squares). The ^{32}P content of Cdc2 was measured with a PhosphorImager after gel electrophoresis.

antibodies in immunoblots as did His6-Xcdc25 protein incubated in M-phase extracts from *Xenopus* eggs (Fig. 3E).

Phosphorylation of Cdc25 by Plx1 modulated the Cdc2-specific phosphatase activity of Cdc25. Treatment of Xcdc25 with His6-Plx1 increased the ability of Xcdc25 to activate Cdc2–cyclin B (Fig. 4A). In control experiments, His6-Xcdc25 treated either with the N172A mutant of His6-Plx1 or with a mock-purified preparation did not undergo activation (Fig. 4A). Moreover, His6-Plx1 did not activate Cdc2–cyclin B in the absence of Xcdc25 (Fig. 4A). His6-Plx1 alone did not phosphorylate histone H1 (Fig. 4A) but did phosphorylate casein (*7*, *25*).

In another assay for Cdc25 activity, we first radiolabeled a recombinant Cdc2–cyclin B complex on Thr^{14} and Tyr^{15} with ^{32}P by treatment with the kinase Myt1 (*26*). His6-Xcdc25 that either had been treated with His6-Plx1 or incubated in an M-phase egg extract was more active in dephosphorylating the complex than was His6-Xcdc25 that either had been treated with the His6-Plx1 N172A mutant or incubated in an interphase egg extract (Fig. 4B).

Our findings indicate that recombinant Plx1 phosphorylates Xcdc25 at multiple sites and regulates its activity. To examine whether this phosphorylation occurs at physiologically relevant sites, we prepared tryptic phosphopeptide maps of His6-Xcdc25 that had been phosphorylated with His6-Plx1, an M-phase *Xenopus* egg extract, or a recombinant Cdc2–cyclin B complex (Fig. 5). The phosphopeptide map of His6-Xcdc25 incubated in M-phase extracts revealed the presence of at least 20 discrete spots. The maps of His6-Xcdc25 phosphorylated by His6-Plx1 or Cdc2–cyclin B yielded at least 10 and 7 tryptic phosphopeptides, respectively. In mixing experiments, we determined that most of the peptides in the maps of His6-Xcdc25 that had been phosphorylated by either His6-Plx1 or Cdc2–cyclin B were also present in the map of His6-Xcdc25 that had been incubated in the M-phase egg extract (*7*). Except for three phosphopeptides, most of the sites phosphorylated by His6-Plx1 did not overlap with those modified by Cdc2–cyclin B. Taken together, these findings indicate that Plx1 phosphorylates Cdc25 at physiologically relevant sites.

Plx1 binds, phosphorylates, and stimulates the phosphatase activity of the Cdc25 protein. Plx1 is related to the Polo family of protein kinases, which have been implicated in mitotic progression in various organisms (*17–20*, *27*). The function of Polo has not been established, but it may regulate the operation of the mitotic spindle. Components of the mitotic spindle and the anaphase-promoting complex become MPM-2 antigens at mitosis (*8*, *9*). Thus, Plx1 may provide a mechanism for coordinating the regulation of Cdc2 with the progression of mitotic processes such as chromosome segregation.

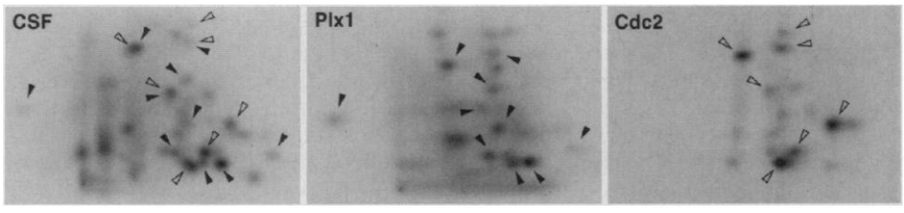

Fig. 5. Phosphopeptide mapping of various phosphorylated forms of Xcdc25. His6-Xcdc25 was phosphorylated in 100 μl of an M-phase extract (CSF) in the presence of 0.5 mCi of [^{32}P]orthophosphate and purified with nickel agarose (top panel). His6-Xcdc25 was phosphorylated in vitro with His6-Plx1 (middle panel) or recombinant Cdc2–cyclin B (bottom panel). In all cases, phosphorylated Xcdc25 was subjected to SDS gel electrophoresis and tryptic phosphopeptide mapping (*24*).

REFERENCES AND NOTES

1. T. R. Coleman and W. G. Dunphy, *Curr. Opin. Cell Biol.* **6**, 877 (1994); W. G. Dunphy, *Trends Cell Biol.* **4**, 202 (1994); R. W. King, P. K. Jackson, M. W. Kirschner, *Cell* **79**, 563 (1994).
2. P. R. Mueller, T. R. Coleman, W. G. Dunphy, *Mol. Biol. Cell* **6**, 119 (1995); P. R. Mueller, T. R. Coleman, A. Kumagai, W. G. Dunphy, *Science* **270**, 86 (1995).
3. A. Kumagai and W. G. Dunphy, *Cell* **70**, 139 (1992).
4. T. Izumi, D. H. Walker, J. L. Maller, *Mol. Biol. Cell* **3**, 927 (1992).
5. K. Galaktionov and D. Beach, *Cell* **67**, 1181 (1991).
6. T. Izumi and J. L. Maller, *Mol. Biol. Cell* **6**, 215 (1995).
7. A. Kumagai and W. G. Dunphy, unpublished results.
8. F. M. Davis, T. Y. Tsao, S. K. Fowler, P. N. Rao, *Proc. Natl. Acad. Sci. U.S.A.* **80**, 2926 (1983); J. Kuang, C. L. Ashorn, M. Gonzalez-Kuyvenhoven, J. E. Penkala, *Mol. Biol. Cell* **5**, 135 (1994).
9. D. D. Vandre, F. M. Davis, P. N. Rao, G. G. Borisy, *Proc. Natl. Acad. Sci. U.S.A.* **81**, 4439 (1984); D. D. Vandre, V. E. Centonze, J. Peloquin, R. M. Tombes, G. G. Borisy, *J. Cell Sci.* **98**, 577 (1991); S. Taagepera, P. N. Rao, F. H. Drake, G. J. Gorbsky, *Proc. Natl. Acad. Sci. U.S.A.* **90**, 8407 (1993); R. W. King *et al.*, *Cell* **81**, 279 (1995); X. S. Ye *et al.*, *EMBO J.* **14**, 986 (1995).
10. J. Kuang and C. L. Ashorn, *J. Cell Biol.* **4**, 859 (1993); J. M. Westendorf, P. N. Rao, L. Gerace, *Proc. Natl. Acad. Sci. U.S.A.* **91**, 714 (1994).
11. Baculovirus transfer vectors encoding histidine-tagged versions of the full-length Xcdc25 protein and its NH_2-terminal domain were prepared by PCR. For full-length Xcdc25, an Nco I site at the initiation codon and a Bgl II site at the end of the coding region were created by PCR amplification of pBluescript-Xcdc25-1 (*3*) with the use of *Pfu* DNA polymerase (Stratagene) and the following oligonucleotides: a, CATGCCATGGCAGAGAGTCACATAATG; and b, GAAGATCTTTAAAGCTTCATTATGCGGGC. The PCR was done for 20 cycles at 94°C for 1 min, 55°C for 2 min, and 75°C for 5 min. For the NH_2-terminal domain of Xcdc25, the procedure was similar except that oligonucleotides a and c (GAAGATCTTTAATT-TAGAAGGGGTCCCG), which created a stop codon at amino acid 265, were used in the PCR reaction. The PCR fragments were ligated into pVL1393-His6 (*28*). Recombinant baculoviruses were generated by standard procedures (Invitrogen), and proteins expressed in Sf9 insect cells were purified with nickel agarose (Pharmacia) (*28*).
12. M-phase extracts from cytostatic factor (CSF)–arrested *Xenopus* eggs were diluted with 2 volumes of extraction buffer (EB) (*3*) containing 1 mM phenylmethylsulfonyl fluoride (PMSF), pepstatin (10 μg/ml), chymostatin (10 μg/ml), and leupeptin (10 μg/ml) and centrifuged at 180,000*g* for 1 hour at 4°C. The supernatant was incubated for 1 hour at 4°C with one-sixth volume of nickel agarose containing 1 mg of His6-Xcdc25-N protein per milliliter of beads. The beads

were washed once with buffer A [10 mM tris-HCl (pH 8.0), 10 μM phosphoserine, 10 μM phosphothreonine, 10 μM phosphotyrosine, 0.1 mM vanadate, and 0.1% CHAPS] containing 500 mM NaCl, 5 mM EGTA, 20 mM β-glycerolphosphate, and 1 μM microcystin. After three additional washes with the same buffer lacking microcystin, bound proteins were eluted from the column with buffer A containing 500 mM NaCl and 200 mM imidazole. The eluate was loaded on a Superdex 200 column equilibrated with buffer A containing 50 mM NaCl, 10 mM EGTA, and 10 mM EDTA. Column fractions containing Xcdc25-specific kinase activity were combined and incubated for 90 min at 4°C with a one-tenth volume of phosphocellulose P11 (Whatman, Hillsboro, OR) prepared as described [Y. Wang and P. J. Roach, in *Protein Phosphorylation: A Practical Approach*, D. G. Hardie, Ed. (IRL Press, Oxford, 1993), pp. 121–144]. The phosphocellulose was washed with 5 volumes of buffer A containing 50 mM NaCl. Bound proteins were eluted in buffer A containing 500 mM NaCl and 20 mM β-glycerolphosphate. The phosphocellulose eluate fraction was dialyzed against buffer A containing 25 mM NaCl and 20 mM β-glycerolphosphate and loaded onto a Mono Q PC 1.6/5 column (Pharmacia) equilibrated in the same buffer. The Mono Q column was eluted with a linear gradient up to 1 M NaCl in the same buffer.

13. The Mono Q fractions containing kinase activity were pooled and loaded onto a 5 to 20% sucrose gradient in buffer A containing 20 mM β-glycerolphosphate. The gradient was centrifuged at 40,000 rpm for 16 hours in a Beckman SW55 rotor at 4°C. The fractions were collected and assayed for Xcdc25-specific kinase activity (*29*).
14. Proteins were separated by electrophoresis and blotted onto Problot (Applied Biosystems). p67 was excised and digested with sequencing-grade trypsin (Boehringer Mannheim) in the presence of hydrogenated Triton X-100 as described [J. Fernandez, L. Andrews, S. M. Mische, *Anal. Biochem.* **218**, 112 (1994)]. The tryptic peptides were separated by reverse phase chromatography in an μRPC C2/C18 2.1/10 column with the use of the SMART system (Pharmacia). Peptide sequence analysis was performed with an ABI 476A sequencer (Applied Biosystems) in the Protein/Peptide Micro Analytical Facility at the California Institute of Technology.
15. Three degenerate primers corresponding to the peptide sequences KKXLX(T/G)TPNYIAPEVL, (A/S)GANTTP, and XX(D/I)APSTIDQ (*30*) were designed: p67-1, AA(A/G)AA(A/G)AA(T/C)(T/C)TITG(T/C)(G/A)(G/C)-IACICC; p67-2, CCAIGGIGTIGT(A/G)TTIGCICC; and p67-3, GCICCI(A/T)(G/C)IA(C/T)IAT(T/C/A)GA(T/C)-CA. X denotes an unreadable amino acid residue. PCR was done with *AmpliTaq* DNA polymerase (Perkin-Elmer), the p67-1 and p67-2 primers, and *Xenopus* oocyte cDNA for 35 cycles at 94°C for 1 min, 45°C for 2 min, and 72°C for 3 min. The reaction yielded a single 850-bp product. A PCR reaction with primer p67-3 indicated that the third peptide sequence was also encoded in the 850-bp fragment.
16. A *Xenopus* oocyte cDNA library in the pAX-NMT vector (*2*) was screened by colony hybridization with the 850-bp PCR fragment that had been labeled in the presence of α-^{32}P–labeled deoxycytidine triphosphate by the random primer method. A Xho I–to–Xho I fragment from the cDNA containing the full coding sequence of Plx1 was subcloned into pBluescript SK$^-$ (pBluescript-Plx1). Plasmids containing nested deletions of the cDNA generated by the Erase-a-base system (Promega Biotech) were sequenced with an ABI 373A automated DNA sequencer (Applied Biosystems).
17. R. M. Golsteyn *et al.*, *J. Cell Sci.* **107**, 1509 (1994); R. Hamanaka *et al.*, *Cell Growth Differ.* **5**, 249 (1994).
18. S. Llamazares *et al.*, *Genes Dev.* **5**, 2153 (1991).
19. H. Ohkura, I. M. Hagan, D. M. Glover, *ibid.* **9**, 1059 (1995).
20. K. Kitada, A. L. Johnson, L. H. Johnston, A. Sugino, *Mol. Cell. Biol.* **13**, 4445 (1993).
21. An Nde I site was created at the initiation codon of Plx1 in a PCR reaction containing *Pfu* DNA polymerase, pBluescript-Plx1 (which contains an internal Nde I site), and the following oligonucleotides: p67-Nde-1, GGAATTCCATATGGCTCAAGTGGCCGG; and p67-Nde-2, CCTATTGACCATATGTCCACTTC. The Nde I–to–Eco RI fragment of pBluescript-Plx1, encoding a COOH-terminal fragment of Plx1, was ligated into pVL1393N-His (*2*). This procedure created pVL-His6-Plx1-C. The PCR fragment was digested with Nde I and ligated into pVL-His6-Plx1-C to yield a baculovirus transfer plasmid encoding the full-length, histidine-tagged Plx1 protein.
22. The catalytically inactive N172A mutant of Plx1 was created by PCR with the following oligonucleotides: p67-N172A-1, AACAGGGCCCCGAGCTTGAGGTC-TCTGTG; and p67-N172A-2, TCGGGGCCCTGTTC-CTTAATGATGAAATGGAGG.
23. For purification of various His6-Plx1 proteins, Sf9 insect cells (2×10^7 cells) were treated for 3 hours with okadaic acid 46 hours after infection. The cells were harvested, washed once with phosphate-buffered saline, and lysed in 1 ml of buffer B [20 mM β-glycerolphosphate, 10 mM Hepes-KOH (pH 7.5), 0.1 mM vanadate, 5 mM EGTA, 5 mM β-mercaptoethanol, 10 μM phosphoserine, 10 μM phosphothreonine, and 10 μM phosphotyrosine] containing 150 mM NaCl, 1% CHAPS, 3 μM microcystin, 1 mM PMSF, pepstatin (10 μg/ml), chymostatin (10 μg/ml), and leupeptin (10 μg/ml). The clarified lysate was incubated with nickel agarose, which was subsequently washed with buffer B (containing 500 mM NaCl and 0.1% CHAPS) and eluted with buffer B (containing 25 mM NaCl and 200 mM imidazole). The eluate was supplemented with 2 mM dithiothreitol (DTT) and 1 mM EDTA and dialyzed against 10 mM Hepes-KOH (pH 7.5), 10 mM NaCl, 1 mM DTT, and 1 mM EDTA for 2 hours at 4°C. Portions were frozen in liquid N_2 and stored at −80°C.
24. W. J. Boyle, P. van der Geer, T. Hunter, *Methods Enzymol.* **201**, 110 (1991).
25. B. Fenton and D. M. Glover, *Nature* **363**, 637 (1993); R. M. Golsteyn, K. E. Mundt, A. M. Fry, E. A. Nigg, *J. Cell Biol.* **129**, 1617 (1995).
26. The Cdc2N133A-Δcyclin B complex, prepared under conditions that allow the phosphorylation of Cdc2 on Thr^{161}, was labeled on Thr^{14} and Tyr^{15} by treatment with the Myt1 kinase as described (*2*).
27. R. Hamanaka *et al.*, *J. Biol. Chem.* **270**, 21086 (1995); K. S. Lee, Y. L. O. Yuan, R. Kuriyama, R. L. Erikson, *Mol. Cell. Biol.* **15**, 7143 (1995).
28. A. Kumagai and W. G. Dunphy, *Mol. Biol. Cell* **6**, 199 (1995).
29. Recombinant His6-Xcdc25 or His6-Xcdc25-N was incubated for 20 min at 23°C with fractions in 20 μl of 5 mM tris-HCl (pH 7.5), 10 mM $MgCl_2$, 1 mM DTT, ovalbumin (0.1 mg/ml), and 50 μM ATP containing 1.6 μCi of [γ-^{32}P]ATP. After incubation, the samples were mixed with gel sample buffer and subjected to SDS gel electrophoresis. In some cases, the reaction was stopped by the addition of 10% phosphoric acid, and portions (10 μl) of each sample were spotted onto P81 phosphocellulose paper (Whatman), which was subsequently washed with 0.5% phosphoric acid. In all cases, the incorporation of ^{32}P into Xcdc25 was quantitated with the use of a PhosphorImager with a known amount of ^{32}P as the standard.
30. Single-letter abbreviations for the amino acid residues are as follows: A, Ala; C, Cys; D, Asp; E, Glu; F, Phe; G, Gly; H, His; I, Ile; K, Lys; L, Leu; M, Met; N, Asn; P, Pro; Q, Gln; R, Arg; S, Ser; T, Thr; V, Val; W, Trp; and Y, Tyr.
31. We thank members of the Dunphy lab for comments on the manuscript, P. R. Mueller for the *Xenopus* oocyte cDNA library, and D. S. Krapf and G. Hathaway for peptide sequencing. Supported in part by a grant from NIH. W.G.D. is an investigator of the Howard Hughes Medical Institute.

15 May 1996; accepted 15 July 1996

A Model of Host-Microbial Interactions in an Open Mammalian Ecosystem

Lynn Bry, Per G. Falk, Tore Midtvedt, Jeffrey I. Gordon*

The maintenance and significance of the complex populations of microbes present in the mammalian intestine are poorly understood. Comparison of conventionally housed and germ-free NMRI mice revealed that production of fucosylated glycoconjugates and an α1,2-fucosyltransferase messenger RNA in the small-intestinal epithelium requires the normal microflora. Colonization of germ-free mice with *Bacteroides thetaiotaomicron*, a component of this flora, restored the fucosylation program, whereas an isogenic strain carrying a transposon insertion that disrupts its ability to use L-fucose as a carbon source did not. Simplified models such as this should aid the study of open microbial ecosystems.

A complex and dynamic microbial ecosystem inhabits the human intestine. Establishment of a microflora begins at birth and progresses through a series of colonizations involving more than 400 bacterial species (*1*). These colonizations result in a metabolically active entity in which anaerobes predominate (*2*). A specific region of the intestine's duodenal-colonic axis will at any given time contain resident (autochthonous) bacterial species and a variable set of transient (allochthonous) species that temporarily occupy a functionally "empty" niche (*3*). Disruption of this open ecosystem—for example, with antibiotics—has revealed the essential role played by the microbiota in preventing infectious diseases (*4*).

The factors that allow components of this indigenous microbiota to establish and maintain their regional habitats are largely unknown. The stability of the ecosystem is all the more remarkable given that the intestinal epithelium is rapidly renewed throughout life (*5*). Integration of the ecosystem into the host may be achieved, at least in part, through dynamic interactions that allow microbes to modify cellular differentiation programs and thus create favorable niches. One way of identifying such programs is by comparing genetically identical mice that (i) have never been exposed to any microorganisms (germ-free, GF), (ii) have been raised with a "normal" functional microbiota (conventional, CONV), and